

# Mechanical Behaviour and Fluid Dynamics Analysis of Metal Hydride for Hydrogen Storage Based on Triply Periodic Minimal Surface Structure

Luthfan Adhy Lesmana\*, Muhammad Aziz

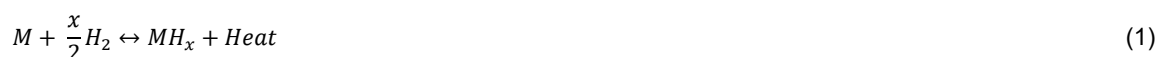
Institute of Industrial Science, The University of Tokyo, 4-6-1 Komaba, Meguro-ku, Tokyo 153-8505, Japan  
[luthfanadhy@g.ecc.u-tokyo.ac.jp](mailto:luthfanadhy@g.ecc.u-tokyo.ac.jp)

Metal hydride (MH) is one of the highly effective hydrogen storage solutions that offer relatively low temperature-pressure working conditions and high volumetric hydrogen density. However, it has a less favorable mobility application due to its gravimetric density. In this study, a triply periodic minimal surface (TPMS) is implemented in the reactor design to withstand the mechanical load. In addition, it can also be adopted as a part of the body frame to compensate for its weight. Reactors are having different wall thicknesses (1, 2, and 3 mm), and TPMS structure types (gyroid, Schwarz D, and Schwarz P) are designed and analyzed to accommodate the same amount of hydrogen storage capacity. The ability to withstand working pressure and load is then investigated with finite element analysis. Pressure drops and heat transfer performance are calculated with computational fluid dynamics (CFD). It is found that using the mobility application scenario, TPMS gyroid with 1mm wall thickness can withstand the working conditions and 5,000 N compressive strength mechanical load. The CFD results also indicated that the fluid inside the proposed gyroid reactor design is swirled and mixed even at a low flow rate with a pressure drop of 325.4 Pa. Based on this finding, TPMS-based structure MH reactor can be considered a promising novel way to store hydrogen in mobility applications.

## 1. Introduction

Hydrogen is found as an economically viable energy storage solution for a wide variety of usage, including the mobility sector (Shin et al., 2019) and stationary scenarios (Gray et al., 2011). Based on its high heating value (HHV), hydrogen has a very high gravimetric energy density (142 MJ/kg), up to three times higher than conventional carbon-based fuels (Mazloomi and Gomes, 2012). However, storing hydrogen in its natural form needs an unpractical amount of space since its volumetric energy density is low. Other storage solutions, like compressed or liquid forms, have safety concerns alongside the economic and energy-intensive disadvantages. Metal hydrides (MHs) are regarded as a feasible method for hydrogen storage because of the superiorities of large volumetric density (Yang et al., 2012) compared to other solutions like liquid and compressed hydrogen. Although MH is considered an excellent candidate to store hydrogen stationarily, there are concerns about the usage of MH in the mobility sector due to its low gravimetric hydrogen density (Lototsky et al., 2017).

MH is formed by a metal compound that experiences the sorption of hydrogen. Pressure-composition-temperature (PCT) relation curve could be used to explain this phenomenon. An initial solid solution of metal ( $\alpha$  phase) is formed just before the hydrogen pressure, and concentration start to increase. MH formation ( $\beta$  phase) starts to form during that condition, and once  $\alpha$  and  $\beta$  phases are in equilibrium, the curve forms a plateau (Nguyen and Shabani, 2021). This reaction can be expressed as Eq(1).



M represents metal/intermetallic alloy, and  $MH_x$  is the MH product with  $x$  acting as a hydrogen ratio. The absorption in MH is an exothermic reaction, while desorption is an endothermic reaction. This leads to saturation in temperature and pressure during the  $\alpha+\beta$  phase; it is required to keep at a certain level so the absorption and desorption reaction can be maintained. In this case, pressure control and thermal management are critical to

keeping reactions occurring. It is correlated strongly to the performance of metal hydride of its capacity and reaction time of storing and releasing hydrogen.

The use of MH offers a viable solution for storing hydrogen with low pressure/temperature conditions, high volumetric density, reversibility of absorption/desorption processes, and high storing safety mechanisms (Lototsky et al., 2017). To facilitate both absorption and desorption of hydrogen, MH needs to be stored at a vessel or reactor. The design of the MH reactor has been found to be important for the storage system to ensure good performance, including capacity (density), reaction time for absorption and desorption, and safety (Harries et al., 2012). Several approaches to increasing the performance of MH has been conducted, including increasing the number of heat exchanger surface area with increasing heat pipes size (Liu et al., 2014), applying fins or extended heat transfer surfaces (Gkanas et al., 2016), and adopting metal foam (Laurencelle and Goyette, 2007).

The process that occurs inside the reactor can be interpreted as governing equations. These equations have been successfully implemented in our previous study (Lesmana and Aziz, 2021), and they consist of the volume-averaged energy balance equation, volume-averaged mass balance equation, and reaction kinetics of MH. Our previous study also implemented a novel way to increase surface area density by adapting TPMS gyroid architecture to further increase the reaction rate of absorption.

TPMS can be generated mathematically from constrained cell shapes patterned asymmetrically in 3D space. The common traits of many forms of this geometric group are that they have two intertwining networks of spaces that also make zero mean curvature. These properties have been used in a heat exchanger (Li et al., 2020), and it has been observed that it can cause large turbulence kinetic energy that is favorable to heat transfer enhancement, although with the cost of high-pressure loss. TPMS that has been classified can be described by using the following expression, which is Schwarz P in Eq(2), gyroid in Eq(3), and Schwarz D in Eq(4). Figure 1 shows the visualization of each equation.

$$\cos(x) + \cos(y) + \cos(z) \quad (2)$$

$$\cos(x) \cdot \sin(y) + \cos(y) \cdot \sin(z) + \cos(z) \cdot \sin(x) \quad (3)$$

$$\sin(x) \cdot \sin(y) \cdot \sin(z) + \sin(x) \cdot \cos(y) \cdot \cos(z) + \cos(x) \cdot \sin(y) \cdot \cos(z) + \cos(x) \cdot \cos(y) \cdot \sin(z) \quad (4)$$

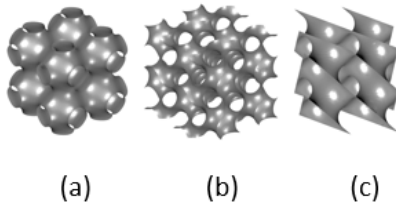


Figure 1: Visualization of (a) Schwarz P, (b) Gyroid, and (c) Schwarz D.

Due to its characteristics, TPMS has been investigated to be applied in many scenarios, like structural engineering (Feng et al., 2019), mass transfer (Thomas et al., 2018), and heat exchanger (Iyer et al., 2022).

The idea of this study comes from current knowledge on both topics in TPMS and MH reactor, which is combining TPMS characteristics and MH reactor design to realize an optimum reactor that could achieve low storing pressure and temperature, high safety, and high energy volumetric density. In addition, it also could be utilized as a load-bearing structure; it can replace the existing structural parts, like the frame and case for the mobility devices (cars or trains). To the authors' best knowledge, there is almost no investigation on MH reactor that implement strength characteristic and the idea of TPMS architecture adaptation for MH reactors, besides the authors' previous works that focus on mathematical kinetics models (Lesmana and Aziz, 2021). Adapting TPMS structure into MH reactor could improve hydrogen storing performance in MH due to the surface area density of TPMS that helps increase heat exchange performance. The capability of TPMS to bear mechanical load also could be utilized to directly reduce the negative effect of low gravimetric density of MH if used as a replacement of frame or structural integrity parts. In this study, mechanical behavior and fluid dynamic analysis are evaluated to determine the capability of the TPMS reactor that is designed to be applicable in most of the frame cases as a cylindrical tube form, with three different wall thicknesses based on three different TPMS architectures, which are Schwarz P, Gyroid, and Schwarz D.

## 2. Method

To determine the capability of the MH reactor that adopts TPMS architecture, a structural mechanic analysis using a finite element method (FEM) and computational fluid dynamics (CFD) are implemented. Samples of the 3D model are prepared using Ansys SpaceClaim, and internal TPMS structures are generated. Each model is generated with the same overall volume (tube shape with dimensions of  $\text{Ø}54 \text{ mm} \times 76 \text{ mm}$ ) and chamber width (12 mm), as shown in Figure 2. Table 1a shows the geometrical properties of the generated model named with model identification (ID) with different TPMS and their properties.

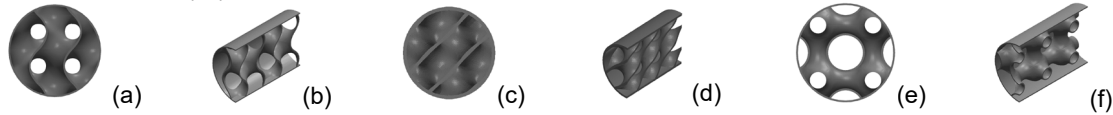


Figure 2: Reactor model generated of (a) gyroid, (c) Schwarz D, and (e) Schwarz P, alongside their respective half-cut section (b, d, and f).

### 2.1 Strength analysis

Based on the previously mentioned models, the mesh model is then composed for each design, as shown in a 1 mm sample of each TPMS design in Figures 3a to 3c. Strength analysis of the reactor is conducted in an ANSYS software package based on FEM. The boundary loads (5,000 N compression load) and fixed support are then applied, as depicted in Figure 3d. Material properties of Al-Si10-Mg (Young modulus of 64 GPa and yield stress of 256 MPa) are adopted since it is the most used material for metal additive manufacturing method (Ishfaq et al., 2021) that is currently considered the only process that could produce TPMS design.

### 2.2 CFD analysis

CFD analysis is conducted with the same model of the reactors. However, to simplify the calculation, the HE liquid boundary is extracted, as shown in Figures 4a to 4c. The governing equations are implemented in this CFD analysis with time-dependent terms of the conservation of mass, momentum, and energy equation. These equations are the built-in function of the Ansys CFX solver. Assumption of constant wall and HE inlet temperature and HE mass flow rate was made.

Fluid flow on this reactor is expected to be turbulent, and, in this case, a time-averaged model is used with Reynolds Averaged Navier Stokes (RANS) equation. Turbulence model of realizable  $k-\epsilon$  model and first-order discretization scheme is chosen in this study. The discretization scheme is selected for pressure, while the first-order upwind scheme is selected for momentum, dissipation rate, and turbulent kinetic energy. Convergence criteria are based on residuals that measure the total imbalance of a conserved variable in each control volume. Boundary conditions, as shown in Table 1b, are assigned in the models based on the scenario of heating MH to represent desorption with the HE temperature profile extracted from the previous study (Lesmana and Aziz, 2021).

To ensure mesh independence results, a mesh independence study is conducted using three grid systems for every model ID on a 1 mm wall thickness variant until no significant changes in the numerical result are observed. Table 2 shows the results from the mesh independence test, and mesh configuration number 2 is selected due to its excellent balance performance between computational cost and numerical accuracy.

Table 1: (a) Reactor design properties and (b) CFD boundary conditions of HE flowing into HE chamber.

Model ID	Wall thickness (h) (mm)	Surface area (mm <sup>2</sup> )	Structural volume (mm <sup>3</sup> )	TPMS MH reactor operating condition	Value
Gyroid_1mm	1	49,971.3	25,372.9	Outlet nozzle pressure	0 (gauge pressure)
Gyroid_2mm	2	46,957.7	47,922.4	Wall temperature (K)	300
Gyroid_3mm	3	44,306.6	68,004.9	Inlet temperature (K)	473.15
SchwarzD_1mm	1	55,789.8	28,067.8	Inlet mass flow rate (m/s)	10
SchwarzD_2mm	2	51,931.7	53,155.2	Fluid	Air
SchwarzD_3mm	3	48,511.4	75,466.7		
SchwarzP_1mm	1	49,984.6	25,261.1		
SchwarzP_2mm	2	48,798.6	54,013.5		
SchwarzP_3mm	3	43,423.9	66,854.1		

Table 2: Mesh independence test results

Model ID	Mesh Configuration Number	Mesh Nodes	Mesh Elements	Average Pressure at Outlet (Pa)
Gyroid_1mm	1	136,545	342,122	1,013.3
	2	98,773	250,289	1,011.4
	3	70,478	184,356	1,412.1
SchwarzD_1mm	1	126,170	423,652	1,432.2
	2	93,408	314,572	1,430.1
	3	82,572	191,485	1,381.1
SchwarzP_1mm	1	127,971	330,693	3,223.3
	2	87,859	219,892	3,243.1
	3	56,535	140,418	3,091.5

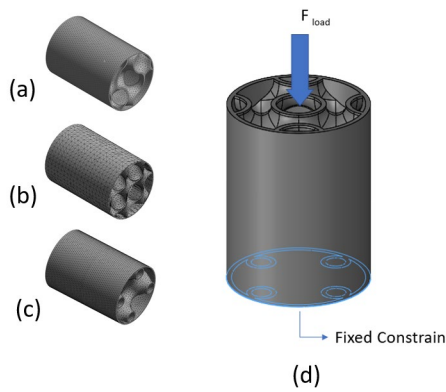


Figure 3. FEM mesh generated for (a) Gyroid\_1mm, (b) SchwarzD\_1mm, and (c) SchwarzP\_1mm. Loads and constrain applied on the model (d)

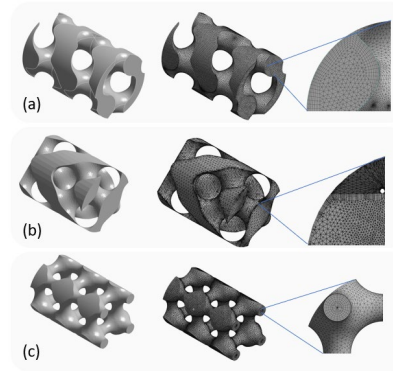


Figure 4. Boundary condition of liquid for CFD analysis extracted from the model of (a) Gyroid\_1mm, (b) SchwarzD\_1mm, and (c) SchwarzP\_1mm with their generated mesh alongside the detailed view on mesh to show the wall boundary layer on outlet side.

### 3. Results and discussion

Based on geometry data and HE fluid chamber volume data, Figure 5 shows the comparison of each model's volume alongside their respective wall thickness. Based on the MH chambers volume, Schwarz D with 1 mm wall thickness shows the highest MH capacity, followed by the same architecture with 2 mm wall thickness. On average, Schwarz D has 22 % higher MH capacity than Schwarz P and 44 % more than gyroid design. It occurs because, during the design process, the symmetrical nature of the TPMS Schwarz D helps in modeling the reactor to strategically position the inlet along with the TPMS pattern so that the amount of MH chamber volume can be maximized.

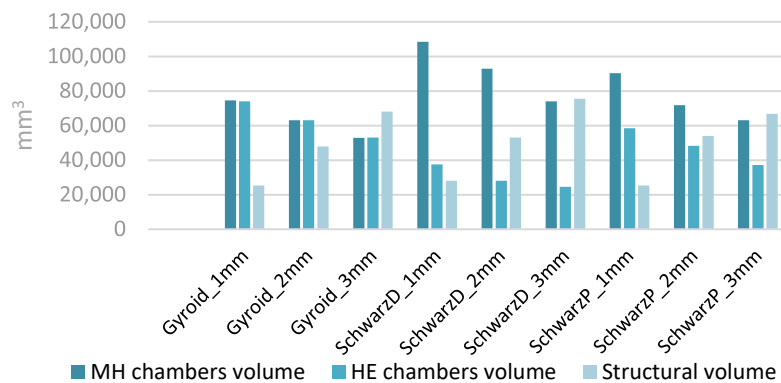


Figure 5. Comparison of volume characteristics of each reactor design.

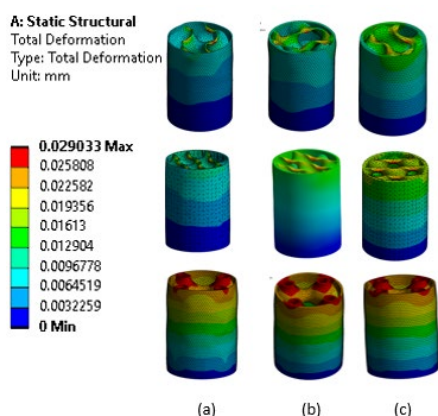


Figure 6. Structural deformation from (a) 1 mm, (b) 2 mm, and (c) 3 mm wall thicknesses of gyroid, Schwarz D, and Schwarz P (from top to bottom) architecture MH reactor.

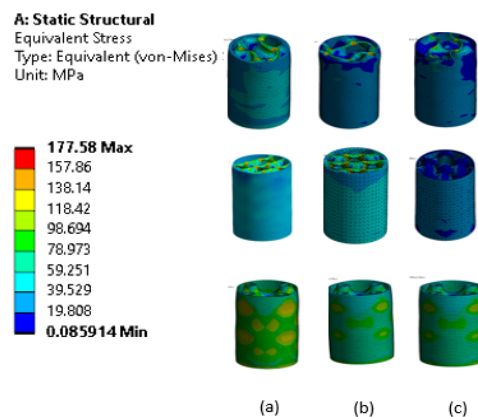


Figure 7. Von-mises distribution from (a) 1 mm, (b) 2 mm, and (c) 3 mm wall thickness of gyroid, schwarz D, and Schwarz P (from top to bottom) architecture MH reactor.

By observing the FEM results from Figures 6 and 7, the risk of material failure can be reduced by adopting a thicker wall. However, the smallest wall thickness that is implemented in this study (1 mm) shows that the proposed model can withstand the applied compressed load. It is also observed that the maximum value of stress is concentrated on the edge of the reactor, especially on the Schwarz P designs.

The results of TPMS upon fluid flow from the CFD analysis are shown in Figure 8. One of the characteristics of TPMS is zero mean curvature that allows the flow to move freely in any direction. The velocity profile shows uniform flow speed across the reactor except on the narrow side of the Schwarz P design, which increases with smaller passages. Furthermore, a noticeable drop in fluid velocity is observed on the Schwarz P design. All velocity profiles and fluid paths show eccentric helical motion on multiple parts of the reactor, with Schwarz P showing the least amount visible. Although this will introduce a pressure drop in higher Reynolds flow, this can enhance the heat transfer that helps the absorption and desorption of hydrogen be sustained so that the reaction rate will increase. Table 3 also shows pressure drop measured from differences in pressure on inlet and outlet for each model ID.

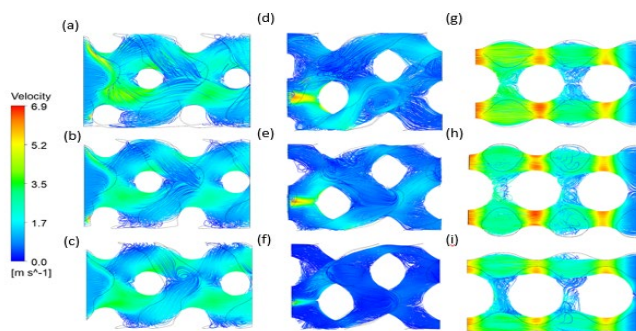


Figure 8. Fluid flow velocity profile of HE liquid in gyroid with (a) 1 mm, (b) 2 mm, and (c) 3 mm wall thicknesses, Schwarz D with (d) 1 mm, (e) 2 mm, and (f) 3 mm wall thicknesses, and Schwarz P with (g) 1 mm, (h) 2 mm, and (i) 3 mm wall thicknesses.

Table 3: Pressure drop of each model

Model ID	Pressure Drop (Pa)
Gyroid_1mm	325.4
Gyroid_2mm	284.7
Gyroid_3mm	213.5
SchwarzD_1mm	218.0
SchwarzD_2mm	198.5
SchwarzD_3mm	186.8
SchwarzP_1mm	116.0
SchwarzP_2mm	108.6
SchwarzP_3mm	93.8

#### 4. Conclusion

Mechanical and HE fluid dynamics behavior of TPMS MH reactor design on gyroid, Schwarz D, and Schwarz P architectures on different wall thicknesses have been numerically evaluated. In this study, the Schwarz P reactor design could store 44 % more than gyroid, but it has the lowest compression load capability and low mixing fluid flow feature with an average velocity of below 1.7 m/s on a 3 mm wall thickness model. A study on pressure drop also shows that due to the straight channel of Schwarz P, the pressure drop shows a lower amount than the other model, only 93.8 Pa on the 3 mm wall thickness design and 116 Pa on the 1 mm design. The gyroid has the lowest MH capacity, but it shows a good performance in mechanical attributes and fluid mixing while

minimizing the decrease of fluid velocity, although it suffers from the highest pressure drop of 325.4 Pa on a 1 mm wall thickness design.

However, to some degree, all the proposed reactor design shows great usability for MH reactor. In addition, the structures of the TPMS MH reactor, which may also be used as a system structure because of its strength, can be manufactured using already accessible manufacturing technologies, such as additive manufacturing. Although the cost of additive manufacturing still becomes the bottleneck for mass production, there has been a promising trend toward cheaper additive manufacturing in the last decade.

The idea of utilizing the TPMS MH reactor for mobile application and adapting it within structural parts, like chassis, cover, and frame, has become a promising solution. It enables further expansion of the hydrogen utilization with safe, high volumetric, and gravimetric densities and energy-efficient TPMS MH hydrogen storage reactor design. Future study of TPMS MH reactor on numerical analysis of kinetics together with thermodynamics of MH and HE liquid that is validated with experimental results to get a real-life performance, such as hydrogen charging and discharging time, becomes further development of this idea.

## References

- Feng J., Fu J., Shang C., Lin Z., Li B., 2019, Sandwich Panel Design and Performance Optimization Based on Triply Periodic Minimal Surfaces, *Computer Aided Design*, 115, 307.
- Gkanas E.I., Grant D.M., Khzouz M., Stuart A.D., Manickam K., Walker G.S., 2016, Efficient Hydrogen Storage in Up-Scale Metal Hydride Tanks as Possible Metal Hydride Compression Agents Equipped with Aluminium Extended Surfaces, *International Journal of Hydrogen Energy*, 41, 10795–10810.
- Gray E.M., Webb C.J., Andrews J., Shabani B., Tsai P.J., and Chan S.L.I., 2011, Hydrogen Storage for Off-Grid Power Supply, *International Journal of Hydrogen Energy*, 36, 654–63.
- Harries D.N., Paskevicius M., Sheppard D.A., Price T.E.C., Buckley C.E., 2012, Concentrating Solar Thermal Heat Storage Using Metal Hydrides, *Proceedings of the IEEE*, 100, 539–49.
- Ishfaq K., Abdullah M., and Mahmood M.A., 2021, A State-of-the-Art Direct Metal Laser Sintering of Ti6Al4V and AlSi10Mg Alloys: Surface Roughness, Tensile Strength, Fatigue Strength and Microstructure, *Optics and Laser Technology*, 143, 107366.
- Iyer J., Moore T., Nguyen D., Roy P., Stolaroff J., 2022, Heat Transfer and Pressure Drop Characteristics of Heat Exchangers Based on Triply Periodic Minimal and Periodic Nodal Surfaces, *Applied Thermal Engineering*, 209, 118192.
- Laurencelle F., Goyette J., 2007, Simulation of Heat Transfer in a Metal Hydride Reactor with Aluminium Foam, *International Journal of Hydrogen Energy*, 32, 2957–2964.
- Lesmana L.A., Aziz M., 2021, Triply Periodic Minimal Surface-Based Heat Exchanger as Metal Hydride Hydrogen Storage Reactor, *Chemical Engineering Transactions*, 88, 229–34.
- Li W., Yu G., Yu Z., 2020, Bioinspired Heat Exchangers Based on Triply Periodic Minimal Surfaces for Supercritical CO<sub>2</sub> Cycles, *Applied Thermal Engineering*, 179, 115686.
- Liu Y., Wang H., Prasad A.K., Advani S.G., 2014, Role of Heat Pipes in Improving the Hydrogen Charging Rate in a Metal Hydride Storage Tank, *International Journal of Hydrogen Energy*, 39, 10552–10563.
- Lototskyy M.V., Tolj I., Pickeing L., Sita C., Barbir F., Yartys V., 2017, The Use of Metal Hydrides in Fuel Cell Applications, *Progress in Natural Science: Materials International*, 27, 3–20.
- Mazloomi K., Gomes C., 2012, Hydrogen as an Energy Carrier: Prospects and Challenges, *Renewable and Sustainable Energy Reviews*, 16, 3024–3033.
- Nguyen H.Q., Shabani B., 2021, Review of Metal Hydride Hydrogen Storage Thermal Management for Use in the Fuel Cell Systems, *International Journal of Hydrogen Energy*, 46, 31699–726.
- Shin J., Hwang W.S., Choi H., 2019, Can Hydrogen Fuel Vehicles Be a Sustainable Alternative on Vehicle Market?: Comparison of Electric and Hydrogen Fuel Cell Vehicles, *Technological Forecasting and Social Change*, 143, 239–48.
- Thomas N., Sreedhar N., Al-Ketan O., Rowshan R., Al-Rub R.K.A., Arafat H., 2018, 3D Printed Triply Periodic Minimal Surfaces as Spacers for Enhanced Heat and Mass Transfer in Membrane Distillation, *Desalination* 443, 256–271.
- Yang F., Cao X., Zhang Z., Bao Z., Wu Z., Serge N.N., 2012, Assessment on the Long Term Performance of a LaNi<sub>5</sub> Based Hydrogen Storage System, *Energy Procedia*, 29, 720–730.